The lymph node transcriptome of unicentric and idiopathic multicentric Castleman disease

Pedro Horna,[1] Rebecca L. King,[1] Dragan Jevremovic,[1] David C. Fajgenbaum[2] and Angela Dispenzieri[3]

[1]Division of Hematopathology, Mayo Clinic, Rochester, MN; [2]Center for Cytokine Storm Treatment & Laboratory, University of Pennsylvania, Philadelphia, PA and [3]Division of Hematology, Mayo Clinic, Rochester, MN, USA

Correspondence: P. Horna
horna.pedro@mayo.edu

Received: November 16, 2021.
Accepted: March 9, 2022.
Prepublished: April 28, 2022.

https://doi.org/10.3324/haematol.2021.280370

Abstract

Castleman disease is a polyclonal lymphoproliferative disorder characterized by unicentric or multicentric lymphadenopathy with characteristic histomorphological features, in addition to variable inflammatory symptomatology. The molecular mechanisms and etiologies of unicentric Castleman disease (UCD) and idiopathic multicentric Castleman disease (iMCD) are poorly understood, and identification of targetable disease mediators remains an unmet clinical need. We performed whole exome sequencing on lymph node biopsies from patients with UCD and iMCD and compared the transcriptomic profiles to that of benign control lymph nodes. We identified significantly upregulated genes in UCD (n=443), iMCD (n=316) or both disease subtypes (n=51) and downregulated genes in UCD (n=321), iMCD (n=105) or both (n=10). The transcriptomes of UCD and iMCD showed enrichment and upregulation of elements of the complement cascade. By immunohistochemistry, C4d deposits indicative of complement activation were found to be present in UCD and iMCD, mostly within abnormally regressed germinal centers, but also in association with plasma cell clusters, endothelial cells and stroma cell proliferations. Other enriched gene sets included collagen organization, S1P3 pathway and VEGFR pathway in UCD; and humoral response, oxidative phosphorylation and proteosome in iMCD. Analysis of cytokine transcripts showed upregulation of *CXCL13* but not *IL6* in UCD and iMCD. Among angiogenic mediators, the VEGFR1 ligand placental growth factor (*PGF*) was upregulated in both disease subtypes. We hereby report for the first time the whole lymph node transcriptomes of UCD and iMCD, underscoring findings that could aid in the discovery of targetable disease mediators.

Introduction

Castleman disease is a rare polyclonal lymphoproliferative disorder resulting in lymph node enlargement with characteristic histopathological features, including germinal center atrophy, hypervasculature, concentric mantle zone hyperplasia, and paracortical plasmacytosis.[1] Most patients (~75-85%) present with a localized lymphadenopathy (unicentric Castleman disease, UCD) that typically resolves with surgical excision, while others (~15-25%) present with multifocal or systemic lymphadenopathy (multicentric Castleman disease, MCD) associated with clinical and laboratory features of a systemic inflammatory response. A subset of cases of MCD is caused by uncontrolled human herpes virus-8 (HHV-8) infection, typically in the setting of human immunodeficiency virus co-infection (HHV-8-associated MCD),[2] while other cases are associated with a plasma cell proliferative disorder and a constellation of clinical and laboratory features known as POEMS syndrome (POEMS-associated MCD).[3] The remaining cases of MCD have heterogeneous clinical manifestations and an unknown etiology (idiopathic multicentric Castleman disease, iMCD). The main unifying feature of Castleman disease is its characteristic lymph node histomorphology on microscopic examination, which can be subclassified into hyaline vascular (most common in UCD), plasmacytic (most common in MCD), and an intermediate or "mixed" variant.[1,4]

The cellular and molecular mechanisms of UCD and iMCD are poorly understood. Most evidence points to an inflammatory process mediated by interleukin (IL)-6, vascular endothelial growth factor (VEGF) and/or chemokines in iMCD,[5,6] compared to a lymphoproliferative process likely mediated by dysregulated lymph node stromal cells in

UCD. However, the etiology of these processes is completely unknown. A few studies have demonstrated the presence of low allele frequency, gene mutations and/or chromosomal abnormalities in a subset of patients with Castleman disease, suggestive of a low-level clonal proliferative process most likely within the stromal cell component.[7-10] While most cases of UCD resolve with surgical excision alone, the treatment of iMCD relies on systemic immunomodulatory therapies aimed at controlling the inflammatory symptomatology. In particular, blockade of IL-6 signaling with anti-IL6 (siltuximab) or anti-IL6 receptor (tocilizumab) antibodies has been shown to result in lasting symptomatic responses, and is currently recommended as the main frontline therapeutic approach. However, two-thirds of patients with iMCD do not respond to anti-IL6 therapy[11] suggesting a heterogeneous biology and the existence of undiscovered disease mediators. Indeed, the lack of other targeted therapies for iMCD remains an unmet clinical need, as this disease is often lifelong, prone to multiple relapses, and associated with significant morbidity and mortality.

We report here for the first time the whole lymph node transcriptomes of UCD and iMCD, in order to generate insights into the pathogenesis of this poorly understood disease and identify potential targets for novel therapeutic strategies.

Methods

Patients' samples and histological review

The laboratory information system at Mayo Clinic (Rochester, MN, USA) was searched for excisional biopsies obtained as clinically indicated between 1992 and 2017, on which residual fresh-frozen tissue aliquots produced for ancillary testing were currently available. All diagnostic pathology material, clinical information and ancillary test results were reviewed to select for cases with a confirmed diagnosis of UCD or iMCD, in addition to cases showing morphologically unremarkable lymph node tissue. We identified and studied 24 lymph node samples from 22 patients with UCD; and seven lymph nodes and one spleen sample from eight patients with iMCD. (Table 1, *Online Supplementary Table S1*). The spleen sample was included based on morphological features similar to those of lymph nodes with iMCD, and clustering of differentially expressed genes together with other iMCD cases (*Online Supplementary Figure S1B*). In addition, we identified 19 control lymph node samples with histomorphological features corresponding to those of unremarkable lymph node tissue, including common slight to moderate-sized germinal centers. These lymph node biopsies were obtained from patients with a history of carcinoma (n=3), lymphoma (n=3), autoimmunity (n=2), orthopedic surgery (n=1), and unexplained lymphadenopathy in the absence of a relevant clinical history (n=10) (*Online Supplementary Table S1*). Cryosections of frozen tissues stained with hematoxylin and eosin (H&E) were reviewed to confirm the specimens' adequacy for exome sequencing. This study was approved by the Mayo Clinic Institutional Review Board.

Histomorphological features of Castleman disease on H&E-stained sections were independently graded by two hematopathologists (PH and RLK) from 0 (absent) to 3 (prominent), based on the five features included in the international diagnostic criteria for iMCD,[4] in addition to three commonly encountered features in UCD (mantle zone hyperplasia, mantle zone rimming, and mantle zone twinning). Discrepant scoring between the two reviewers was averaged to the nearest integer number. None of the samples had morphological evidence of a dendritic or stromal cell neoplasm, although two cases of UCD showed marked stromal proliferation. All cases of iMCD met international diagnostic criteria,[4] including lymphadenopathy in two or more lymph node stations, negativity for HHV-8 by immunohistochemistry for latency-associated nuclear antigen (LANA-1), lack of immunoglobulin light chain-restriction on plasma cells by immunohistochemistry for kappa and lambda, no evidence of an infectious, neoplastic or autoimmune process; and consistent clinical, laboratory and imaging findings. Peripheral neuropathy was documented in only one patient (in the absence of a plasma cell proliferative disorder), and thrombocytopenia was present in another single patient who also had anasarca in the setting of cardiovascular comorbidities.

Exome sequencing

Total RNA was extracted from cryosections of residual O.C.T.-embedded/fresh-frozen biopsy aliquots, using miRNeasy Mini Kit (Qiagen, Germantown, MD, USA) and a QIAcube automated handler (Qiagen). RNA quality and concentration were assessed on an Agilent 2100 Bioanalyzer (Agilent Technologies, Santa Clara, CA, USA) and a NanoDrop 200 spectrophotometer (Thermo Fisher Scientific, Waltham, MA, USA), respectively. cDNA libraries were prepared using TruSeq Stranded mRNA Sample Prep Kit (Illumina, San Diego, CA, USA), and quality was checked on an Agilent 2100 Bioanalyzer (Santa Clara, CA, USA) and Qubit 4 fluorometer (Invitrogen, Carlsbad, CA, USA). Libraries were amplified on an Illumina CBot automated cluster generator and sequenced as 100 X 2 paired end reads on an Illumina HiSeq 4000. Sequences were aligned using MAP-RSeq version 3.1.2[12] and processed with the Subread package[13] to produce normalized counts as fragments per kilobase of transcript per million mapped fragments (FPKM) (*Online Supplementary Figure S1A*).

Table 1. Demographic and histomorphological characteristics of the samples studied.

	Control lymph node	UCD	iMCD	*P* value
Number	19	24	8	-
Age in years, mean ± SD	49 ± 21	46 ± 18	53 ± 11	-
Sex male : female	0.6:1	0.6:1	2.3:1	-
Location of tissue sampled, N (%)				
Superficial	15 (75)	6 (25)	7 (88)	<0.001
Deep	4 (21)	18 (75)	1 (12)	
Sampled tissue, N (%)				
Cervical LN	9 (47)	3 (13)	2 (25)	
Axillary LN	5 (26)	3 (13)	5 (63)	
Inguinal LN	1 (5)	0 (0)	0 (10)	
Mediastinal LN	0 (0)	4 (17)	0 (0)	-
Abdominal LN	1 (5)	3 (13)	0 (0)	
Retroperitoneal LN	2 (11)	8 (33)	0 (0)	
Pelvic LN	1 (5)	2 (8)	0 (0)	
Other	0 (0)	1 (4)	1 (13)	
Histological variant, N (%)				
Hyaline vascular	-	20 (83)	0 (0)	<0.0001
Plasmacytic or mixed	-	4 (17)	10 (100)	
Histological scoring [0-3], mean ± SD				-
Regressed GC	0.2 ± 0.4	3.0 ± 0	2.0 ± 0.9	<0.0001
FDC prominence	0.0 ± 0.0	1.9 ± 0.8	1.0 ± 0.9	<0.0001
Increased vascularity	0.5 ± 0.7	2.5 ± 0.6	1.3 ± 1.0	<0.0001
Hyperplastic GC	1.3 ± 0.7	0.5 ± 0.5	1.6 ± 1.4	<0.001
Plasmacytosis	0.1 ± 0.3	0.7 ± 1	2.4 ± 0.5	<0.0001
MZ hyperplasia	0.1 ± 0.3	2.0 ± 1	1.0 ± 0.8	<0.0001
MZ rimming	0.1 ± 0.3	2.1 ± 0.9	1.4 ± 1.4	<0.0001
MZ twinning	0.1 ± 0.2	1.9 ± 1.0	0.5 ± 0.8	<0.0001
Total histological score [0-24],mean (range)	1.5 (0-5)	14.6 (10-19)	11.1 (8-18)	<0.0001

UCD: unicentric Castleman disease; iMCD: idiopathic mutlicentric Castleman disease; SD: standard deviation; LN: lymph node; GC: germinal center; FDC: follicular dendritic cell; MZ: mantle zone.

Differential gene expression and gene set enrichment analysis

Analysis of differentially expressed genes and gene set enrichment was performed using Qlucore Omics Explorer v. 3.7 (Qlucore, Lund, Sweden). A cutoff of 0.5 FPKM was applied to filter out rare transcripts, and expression values were $\log_2$-transformed. Differentially expressed genes were studied separately for UCD *versus* controls, and iMCD *versus* controls (two-sample *t*-test). *P*-values were adjusted for multiple testing using the Benjamini-Hochberg method,[14] and genes with adjusted *P*-values below 0.01 (resulting in q<0.05 for UCD, and q<0.1 for iMCD) and greater than a 2-fold change were considered as differentially expressed. The distribution of samples based on gene expression was visualized on a three-dimensional principal component analysis plot, after filtering out variables with low variance to reduce noise based on the previously reported projection score.[15] In addition, sample outliers were studied on a *t*-distributed stochastic neighbor embedding (t-SNE) plot of differentially expressed genes (3-group analysis of variance [ANOVA], *P*<0.001, q<0.01).

Gene set enrichment analysis (GSEA)[16] was performed separately for UCD *versus* controls, and iMCD *versus* controls, using gene set permutation, a statistical significance of *P*<0.05 and q<0.05, and the following gene set lists downloaded from MSigDB (*https://www.gsea-msigdb.org*, accessed 08/18/2021): Hallmark gene sets, Kyoto Encyclopedia of Genes and Genomes (KEGG) pathways, Pathway Interaction Database (PID), Gene Ontology-Biological Process (GO-BP), and Gene Ontology-Molecular Function (GO-MF). In addition, differentially expressed genes corresponding to arbitrarily selected gene sets of interest were separately captured using a 2-fold change threshold and a statistical significance of *P*<0.05 (q<0.2).

Immunohistochemistry

Formalin-fixed/paraffin-embedded tissue sections were immunostained on a Benchmark XT autostainer (Ventana Medical Systems, Inc, Tucson, AZ, USA), using a primary anti-C4d rabbit polyclonal antibody (catalog #: 12-5000; American Research Products, Belmont, MA; USA) or a primary anti-CXCL13 mouse monoclonal antibody (clone 53610; R&D systems, Minneapolis, MN, USA), as previously described.[17,18]

Other statistical analyses

Demographic, specimen and histomorphological characteristics were compared between groups using one-way ANOVA for continuous variables, the χ^2 test for most nominal values, Fisher exact test for nominal values with small samples, and Kruskal-Wallis test for ordinal variables. *P* values <0.05 were considered statistically significant. Statistical analyses and bar plots were performed on GraphPad Prism v. 9.1.0 (GraphPad Software, San Diego, CA, USA).

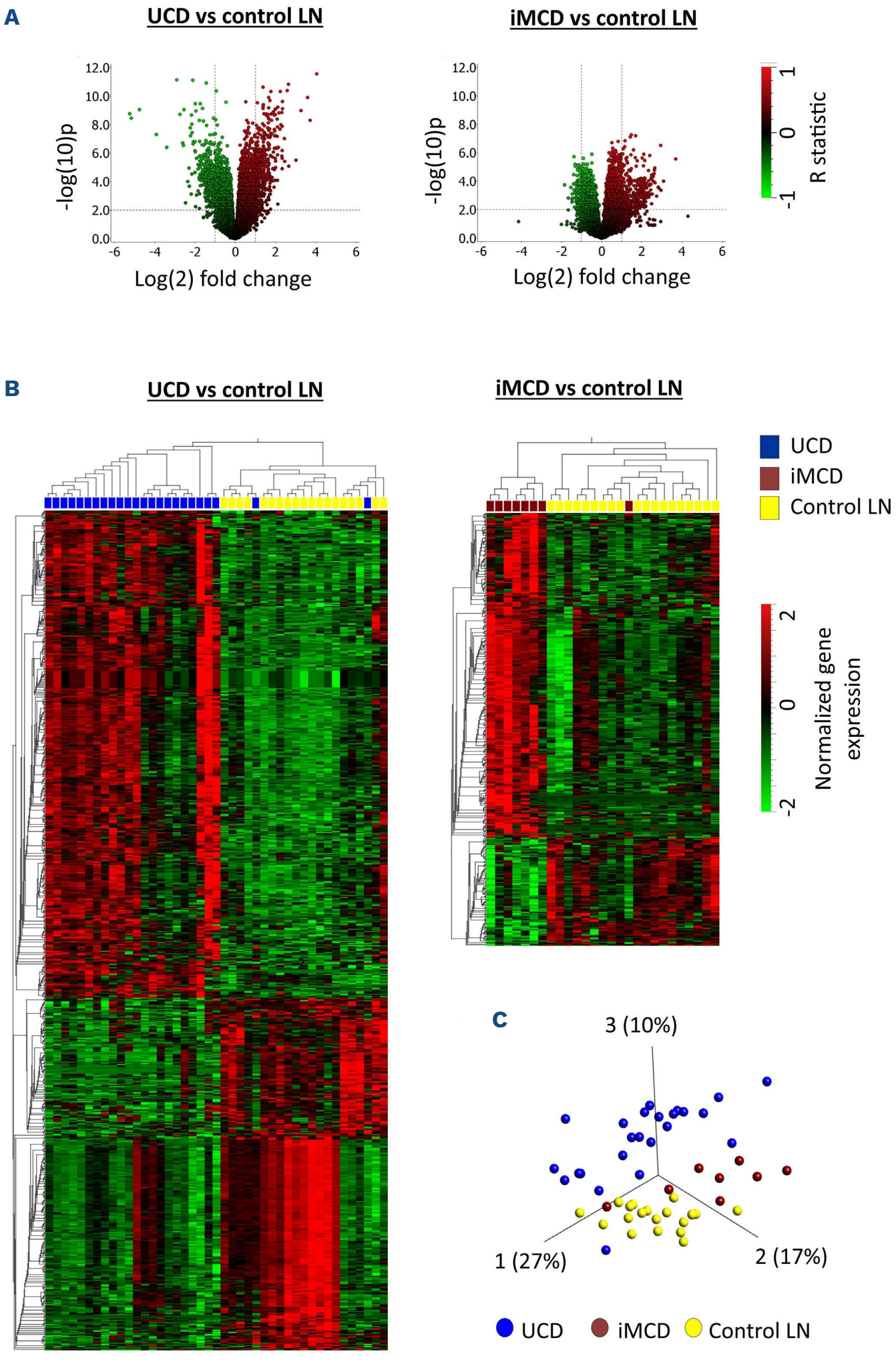

Continued on following page.

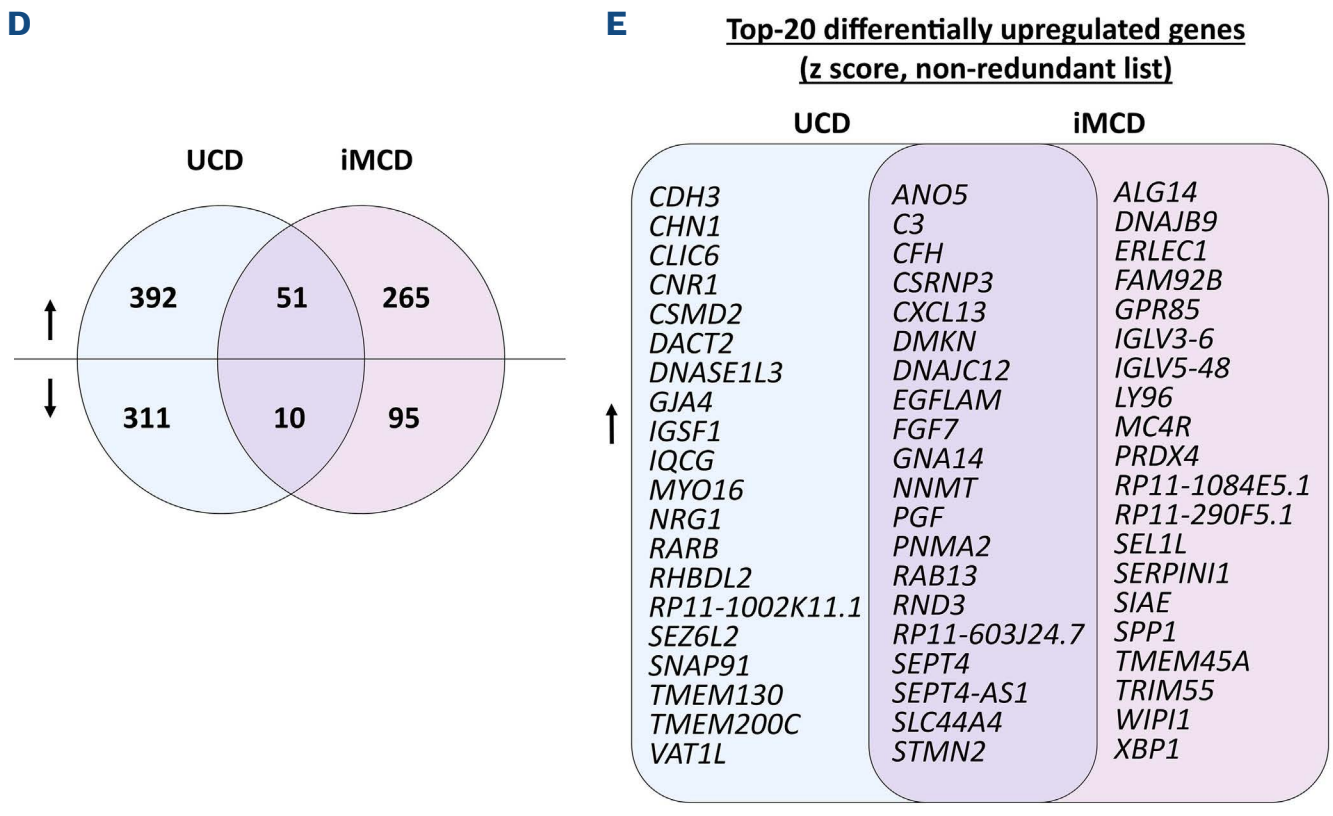

Figure 1. The gene expression profiles of unicentric and idiopathic multicentric Castleman lymphadenopathy are distinct from that of control lymph nodes. (A). Volcano plots showing divergent gene expression compared to that of control lymph nodes (control LN), for cases of unicentric Castleman disease (UCD, left) and idiopathic multicentric Castleman disease (iMCD, right). Dotted lines depict arbitrary thresholds for differential gene expression of 2-fold difference (vertical) and $P<0.01$ (horizontal). (B) Heatmap of differentially expressed genes displayed in a two-way hierarchical clustering arrangement. (C) Three-dimensional principal component analysis plot based on the expression of 1,027 highly variant genes across all samples. (D) Venn diagram of the number of differentially upregulated (upward arrow) or downregulated (downward arrow) genes in UCD, iMCD and both. (E) Top 20 upregulated genes in UCD (left), iMCD (right) and both (middle) based on Z-score, shown as non-redundant gene lists in alphabetical order.

Results

The transcriptome of Castleman lymphadenopathy is distinct from that of control lymph nodes and differs between unicentric and multicentric disease

Whole exome sequencing performed on frozen lymph nodes from patients with UCD and iMCD revealed statistically significant differences in the expression of multiple genes, when compared to the expression in control lymph nodes (Figure 1). Overall, 443 and 316 genes were upregulated (>2 fold, $P<0.01$) in UCD and iMCD, respectively, with 51 genes upregulated in both disease subtypes compared to controls. Similarly, 321 and 105 genes were downregulated in UCD and iMCD, respectively, with ten genes downregulated in both disease subtypes (Figure 1D, E). Principal component analysis based on 1,027 highly variant genes across samples showed segregation of UCD, iMCD and control lymph node specimens, with few overlaps (Figure 1C). Thus, the transcriptomic profiles of lymph nodes from patients with UCD and iMCD were different from the profile of control lymph nodes, and also different from each other.

Gene sets enriched in UCD included collagen fibril organization and related pathways, in addition to the sphingosine 1-phosphate receptor 3 (S1P3) pathway previously described as a mediator of fibrosis[19] (Table 2, *Online Supplementary Data S1*). Genes related to cell cycle and DNA replication were underrepresented in UCD, perhaps due to the paucity of proliferating germinal center B-cells within the characteristically depleted B cell follicles. In iMCD, the transcriptome enrichment was dominated by gene sets with potential relationship to the commonly encountered plasmacytic infiltrates (humoral immune response, proteosome, protein N-linked glycosylation)[20,21] (Table 2), including elements of the electron transport chain possibly related to the known increased oxidative metabolism of plasma cells.[22] The transcriptome of iMCD was also enriched for genes upregulated by mTOR complex 1 activation, a signaling pathway central to protein synthesis, cellular proliferation and metabolism,[23] recently identified to be upregulated in lymph nodes and enriched in serum proteins from patients with iMCD.[24,25] Genes related to T-cell signaling were underrepresented in both UCD and iMCD.

Enrichment for elements of the complement cascade characterize both unicentric and multicentric Castleman lymphadenopathy.

GSEA was consistent with upregulation of transcripts related to the complement cascade in both UCD and iMCD (Table 2). Genes that showed a greater than 2-fold increase with statistical significance ($P<0.05$) included the

Table 2. Selected pathways and gene ontologies enriched in the transcriptome of Castleman lymphadenopathy.

Disease subtype	Trend	Annotation	Gene set	NES
Unicentric	Up	COMPLEMENT AND COAGULATION CASCADES	KEGG	2.11237
		COLLAGEN FIBRIL ORGANIZATION	GOBP	2.09074
		S1P S1P3 PATHWAY	PID	2.05938
		VEGFR SIGNALING PATHWAY	GOBP	2.05778
	Down	T HELPER 17 CELL LINEAGE COMMITMENT	GOBP	-1.88912
		REGULATORY T CELL DIFFERENTIATION	GOBP	-2.15572
		CD8 TCR PATHWAY	PID	-2.16138
		CELL CYCLE	KEGG	-2.42726
		DNA REPLICATION	KEGG	-2.5918
Multicentric	Up	HUMORAL IMMUNE RESPONSE	GOBP	2.72929
		RESPIRATORY ELECTRON TRANSPORT CHAIN	GOBP	2.65332
		PROTEIN N LINKED GLYCOSYLATION	GOBP	2.64169
		OXIDATIVE PHOSPHORYLATION	KEGG	2.59304
		PROTEASOME	KEGG	2.45512
		COMPLEMENT AND COAGULATION CASCADES	KEGG	2.25133
		ANTIGEN PROCESSING AND PRESENTATION	GOBP	1.94522
		MTORC1 SIGNALING	HALLMARK	1.90294
		INTERLEUKIN 1 MEDIATED SIGNALING PATHWAY	GOBP	1.8716
	Down	T CELL RECEPTOR SIGNALING PATHWAY	KEGG	-2.32199

P<0.05 and q<0.05 for all enrichments. See *Online Supplementary Data S1* for the complete list. NES: normalized enrichment score; KEGG: Kyoto Encyclopedia of Genes and Genomes; GOPB: Gene Ontology-Biological Process; PID: Pathway Interaction Database.

main complement effector *C3* in both UCD and iMCD as well as core components of the classic complement pathway *C1S* and *C1R* in UCD, and *C4A* and *C4B* in iMCD (Figure 2A). *C4BPA* and *CFH* transcripts were also increased in both unicentric and multicentric disease, the products of which are known regulators of the classical and alternative complement pathways, respectively. Other related findings include upregulation of the inhibitors of plasminogenesis *SERPINE1* (plasminogen activator inhibitor 1) and *SERPINF2* (α2 antiplasmin) in unicentric disease, and *SERPINA5* (protein C inhibitor) and *A2M* (α2 macroglobulin) in multicentric disease; with potential to modulate the complement cascade given the role of plasmin as a complement regulator.[26]

Given the enrichment of the complement pathway via the whole transciptome, we sought to apply an orthogonal approach to confirm complement activation in lymph node tissue and to identify sites of complement activation in UCD and iMCD. We performed immunohistochemistry on histological sections to detect C4d, an end-product of C4 commonly utilized as a biomarker of activation of the classical and/or lectin complement pathways.[27] Most control lymph nodes (14 of 19 cases, 74%) showed only faint to variable staining for C4d within the dendritic cell meshworks of germinal centers (Figure 3A, D), while a subset of cases (n=4, 21%) showed strong staining within the light zone of germinal centers (Figure 3G). In contrast, most cases of UCD (14 of 24, 58%) showed strong expression of C4d within the regressed germinal centers and extending into the abnormally expanded mantle zones in a “flame-like” pattern (Figure 3B). One additional case of “stromal-rich” UCD showed strong C4d expression within abundant spindle-appearing cells (likely stromal or dendritic cells) (Figure 3H), while two other cases showed C4d expression on endothelial cells (Figure 3E) or clusters of plasma cells. Of the eight cases of iMCD studied, five (63%) showed strong C4d expression within germinal centers (with variable extension into mantle zones) (Figure 3C), one case showed strong expression within both germinal centers and paracortical plasma cell clusters (Figure 3I), and two cases showed scattered C4d-positive paracortical plasma cells only (Figure 3F). Overall, the findings are suggestive of complement activation in both UCD and iMCD, mostly occurring within or adjacent to the follicular dendritic cell processes of abnormal B-cell follicles, but also occasionally in association with clusters of plasma cells, endothelial cells or atypical stromal cell proliferations.

Upregulated immune-related transcripts in Castleman lymphadenopathy include CXCL13 and selected cytokines, but not interleukin-6

Given that cytokines are known to be upregulated in the serum of iMCD patients, we decided to investigate which cytokines had increased gene expression within the lymph node tissue (Figure 2B). The most distinctively upregulated cytokine in UCD was *SCG2* (secretogranin II), the precursor of the multifunctional protein secretoneurin which has chemotactic effects on leukocytes and fibroblasts.[28] In iMCD, the most distinctively upregulated cytokine was *SPP1* (osteopontin), a multifunctional matricellular protein with pro-inflammatory properties on macrophages, dendritic and other immune cells.[29-31] Unexpectedly, *IL6* transcripts were not increased in lymph nodes of UCD or iMCD patients compared to controls (P=0.5, fold change = 1.3, for both comparisons).

The B lymphocyte chemoattractant *CXCL13* was upregulated in both UCD and iMCD. To study the sites of CXCL13 production in the lymph node, we performed immunohistochemistry for CXCL13 on histological sections. As previously described,[18,32,33] CXCL13 expression in control lymph nodes was exclusively restricted to B-cell follicles, and present mostly on scattered lymphoid-appearing round cells within reactive germinal centers, likely representing T follicular helper cells (Figure 3J), in addition to few spindle-appearing cells within the germinal centers and mantle zones, likely representing follicular dendritic cells. In contrast, CXCL13 staining in cases of UCD and iMCD showed expression mostly on the concentrically arranged follicular dendritic cells within regressed germinal centers, in addition to scattered follicular dendritic cells within expanded mantle zones (Figure 3K, L). A few T-follicular helper cells within normal-appearing germinal centers in iMCD were also positive for CXCL13.

Upregulated angiogenic mediators in Castleman lymphadenopathy include VEGFR1 (FLT1) and its lesser known ligand placental growth factor

Given that increased vascularity is commonly observed in lymph nodes involved by UCD and iMCD (Table 1), and that serum VEGF is commonly increased in patients with iMCD,[34] we decided to study the differential expression of genes related to angiogenesis in our cohort. Genes associated with the VEGF receptor (VEGFR) signaling pathway were enriched in UCD but not in iMCD (Table 2). In UCD, *VEGFR1* (FLT1) and its lesser known ligand placental growth factor (*PGF*) were both differentially upregulated

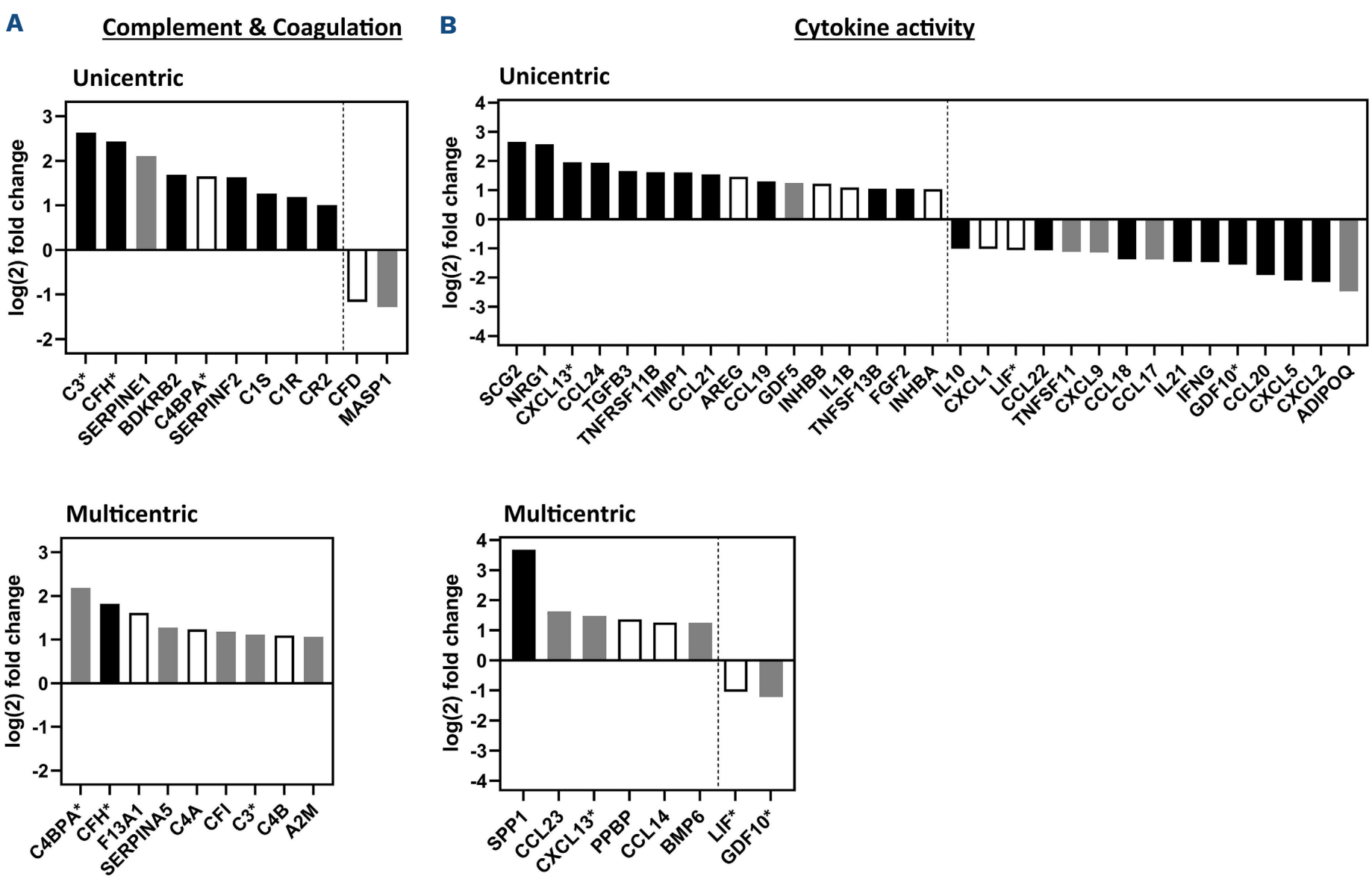

Continued on following page.

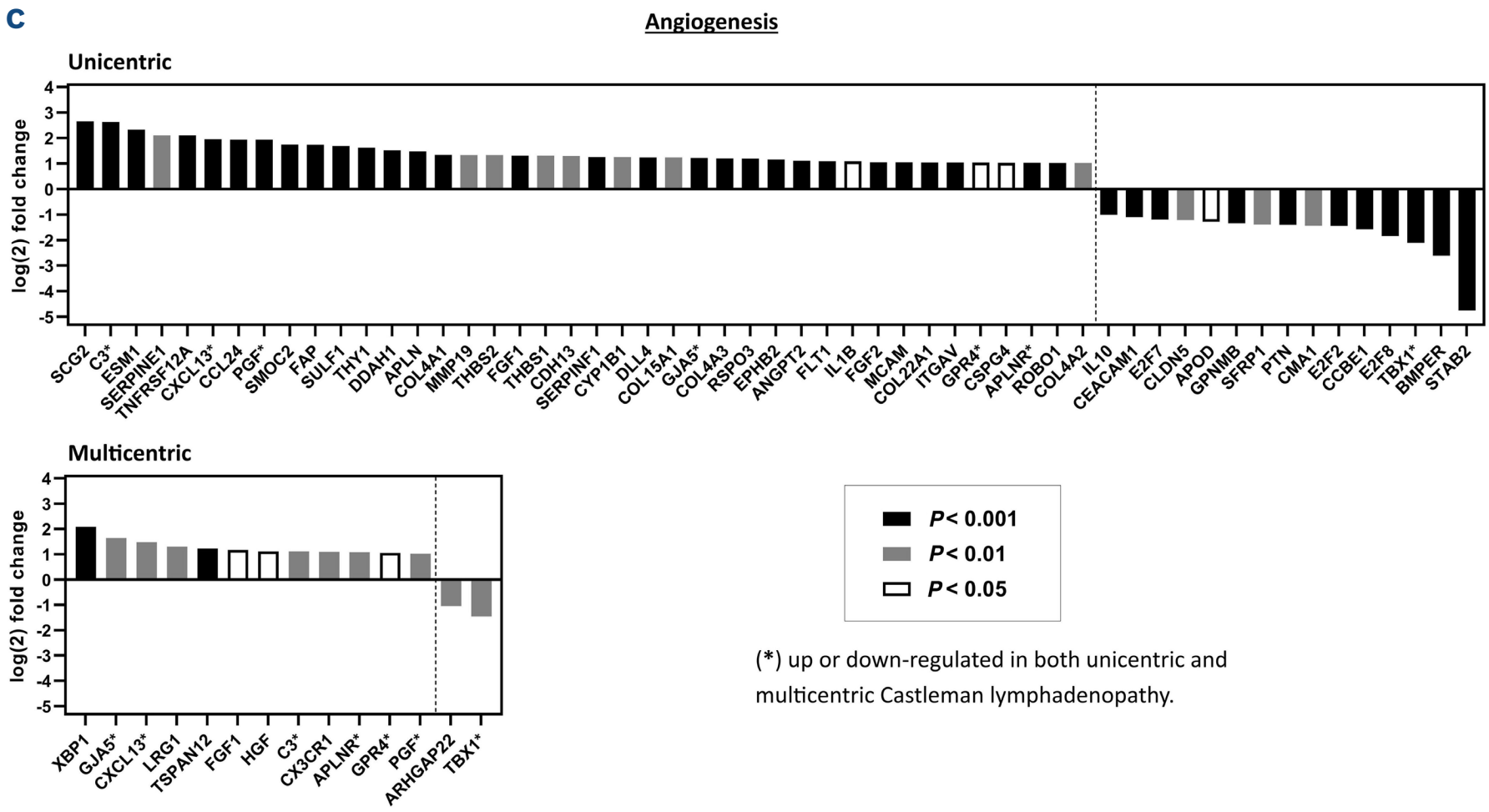

Figure 2. The lymph node transcriptome of Castleman disease includes upregulation of elements of the complement cascade, and a distinct cytokine and angiogenic profile. Bar plots show upregulated or downregulated genes corresponding to selected gene sets in unicentric (upper plots) and multicentric (lower plots) Castleman disease, based on a greater than 2-fold difference and a statistical significance of $P<0.001$ (black bars), $P<0.01$ (gray bars) or $P<0.05$ (white bars). Genes upregulated or downregulated in both unicentric and multicentric disease are highlighted with (*). (A) "Complement and coagulation cascades" gene set from the Kyoto Encyclopedia of Genes and Genomes (KEGG). (B) "Cytokine activity" gene set (GO:0005125) from gene ontology (GO) analysis. (C) "Angiogenesis" gene set (GO:0001525) from GO analysis.

(Figure 2C). Of the two other VEGR1 ligands,[35] *VEGFA* was significantly upregulated ($P<0.05$, $q<0.1$) but below the 2-fold arbitrary threshold for differential expression (fold change =1.7), while *VEGFB* transcripts were not significantly different from controls ($P=0.09$). In addition, apelin receptor (*APLNR*) and its ligand apelin (*APLN*), both important mediators of pathological angiogenesis,[36] were differentially upregulated in UCD. In iMCD, *PGF* was also differentially upregulated (Figure 2C), and its receptor *VEGFR1* was likewise significantly increased ($P<0.05$, $q<0.1$) but below the 2-fold arbitrary threshold for differential expression (fold change = 1.8). *APLNR* was also differentially upregulated in iMCD, but not its ligand *APLN* ($P=0.3$). Transcripts for *VEGFA* and *VEGFB* were not significantly different between iMCD and controls ($P=0.1$ and $P=0.7$, respectively). Overall, the findings mirrored the more prominent vascularity observed microscopically in UCD compared to iMCD (Table 1), with possible common angiogenic pathways involving PGF/VEGFR1 and APLN/APLNR.

Discussion

Here, we describe the transcriptome of lymph nodes from patients with UCD and iMCD. Our study demonstrates that the transcriptome of Castleman lymphadenopathy is distinct from that of control lymph nodes, and different between unicentric and multicentric disease (Figure 1C). Many of these differences mirror the characteristic histopathological features of Castleman lymphadenopathy, including increased collagenous fibrosis, increased vascularity and a paucity of proliferating germinal center B cells in UCD; and paracortical plasmacytic infiltrates in iMCD (Table 2). The underrepresentation of genes associated with T-cell signaling in UCD and iMCD (Table 2) needs to be further studied, but is consistent with a histomorphology suggestive of abnormal B-cell and plasma cell immunity, in the absence of prominent T-cell infiltrates.

We demonstrate that the transcriptomes of both UCD and iMCD are enriched for elements of the complement cascade. For the first time, we showed that complement activation in lymph nodes affected by Castleman disease occurs most commonly within the abnormally regressed germinal centers and expanded mantle zones. The complement cascade plays a critical role in the normal function of germinal centers, which are known to be dysregulated in Castleman disease. Complement-coated antigens are captured and retained by follicular dendritic

cells expressing complement receptors 1 (CD35) and 2 (CD21), facilitating recognition by antigen-specific B-cell receptors expressed by germinal B cells. In addition, modulation of the cell surface complement regulators CD55 and CD59 by germinal center B cells results in production of the complement-derived anaphylotoxins C3a and C5a which are crucial for germinal center B-cell activation and differentiation towards plasma cells, while preventing the generation of the cytotoxic complement-derived membrane attack complex.[37] The increased transcription of complement-related genes in Castleman lymphadenopathy and evidence of complement activation within the characteris-

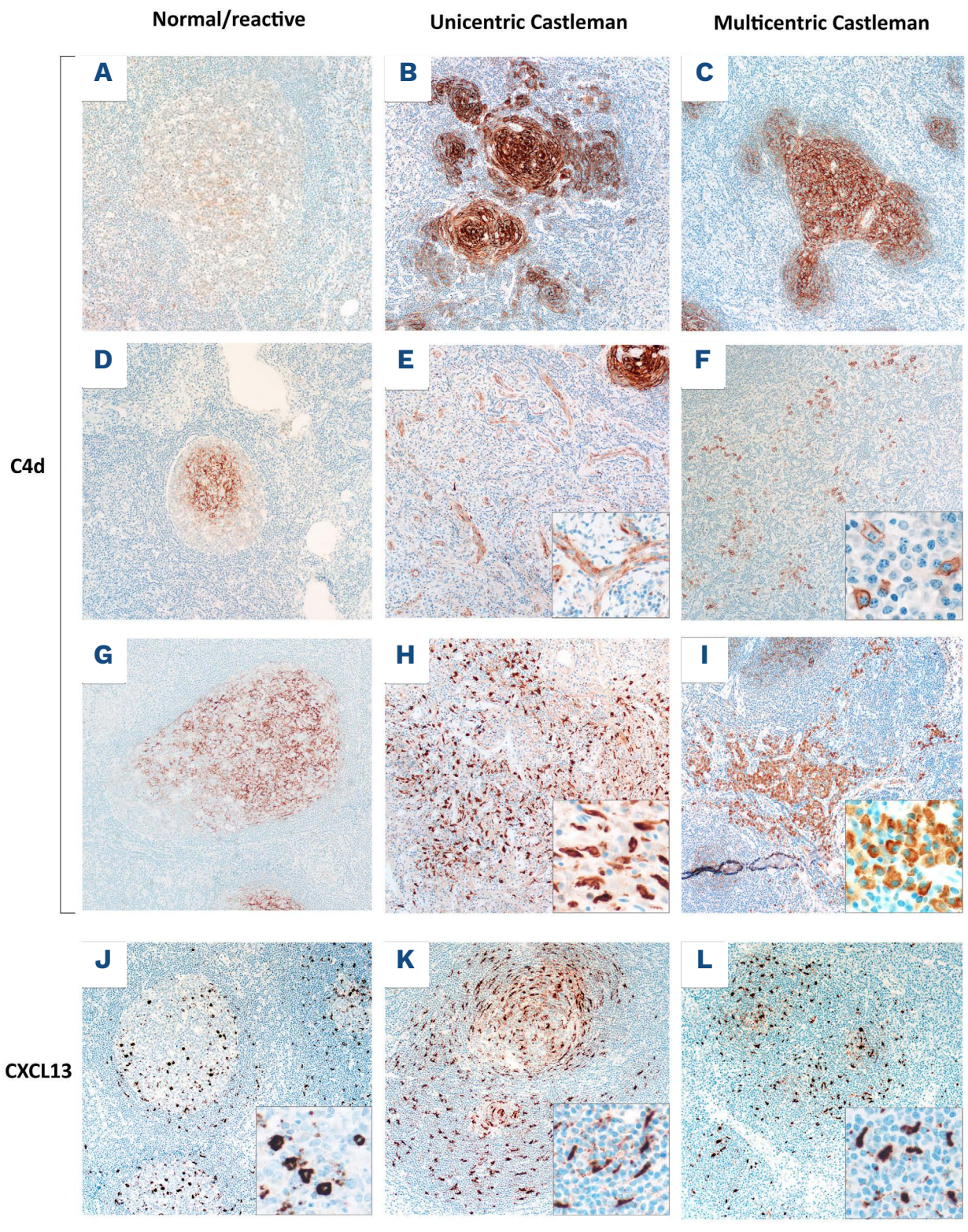

Figure 3. Histological localization of complement activation and CXCL13 production in lymph nodes involved by Castleman disease. In most control lymph nodes, immunohistochemistry for C4d (upper 3 rows) showed only focal and faint complement activation within germinal centers (A, D), with a few cases showing more robust activation within the germinal center light zone (G). In contrast, most cases of unicentric Castleman disease (UCD) showed marked complement activation on germinal centers and extending into the mantle zone in a "flame-like" pattern (B). In addition, some UCD cases showed C4d staining on endothelial cells (E) and, rarely, on expanded stromal cells (H) or plasma cells (*not shown*). Similarly, most cases of idiopathic multicentric Castleman disease (iMCD) showed strong C4d staining within germinal centers (C), in addition to positive staining on small (F) or large (I) clusters of plasma cells in a subset of cases. Immunohistochemistry for CXCL13 in control lymph nodes predominantly highlighted small lymphocytes within and around germinal centers (T follicular helper cells) (J), in addition to a less conspicuous positivity on a few scattered spindle cells (follicular dendritic cells). In contrast, CXCL13 staining on regressed B-cell follicles in UCD (K) and iMCD (L) predominantly highlighted spindle cells (follicular dendritic cells) concentrically arranged within atrophic germinal centers and scattered throughout expanded mantle zones. Microphotographs were obtained at 100X (main) or 400x (insets) total magnification.

tically abnormal germinal centers raise the possibility of complement activation as a possible mediator of the inflammatory manifestations of UCD and iMCD.

Interestingly, transcripts of the B-cell attracting chemokine *CXCL13* were increased in both UCD and iMCD. Immunohistochemistry localized this chemokine largely to follicular dendritic cells within the abnormal germinal centers. Our findings are consistent with a prior study showing that CXCL13 is the most upregulated blood chemokine during flares of iMCD, and that there is increased tissue expression of CXCL13 in iMCD germinal centers.[6] CXCL13 is essential for B-cell homing to germinal centers, and its increased production has been regarded as a biomarker of germinal center activity and development of B-cell immunity.[38] However, CXCL13 can also be produced by T follicular helper cells, which appear to be the predominant CXCL13-positive population in our control lymph nodes and other similar studies.[33] In contrast, the characteristically abnormal B-cell follicles of Castleman disease appear to be largely devoid of CXCL13-positive T follicular helper cells, with most of the CXCL13 protein expression originating from follicular dendritic cells. Thus, increased B-cell homing to lymph nodes through upregulation of *CXCL13* in addition to an abnormal balance of CXCL13 production by follicular dendritic cells *versus* T follicular helper cells could both be important factors in the pathogenesis of Castleman disease.

We did not find increased *IL6* transcripts on lymph nodes from patients with Castleman disease, compared to controls. This finding was unexpected, as the inflammatory manifestations of Castleman disease are believed to be mediated at least in part by IL-6, based on several lines of evidence. High levels of serum IL-6 in patients with iMCD are associated with increased disease activity.[34,39] In transgenic mice, overexpression of IL-6[40] or the HHV8-encoded vIL6[41] results in an extensive accumulation of polytypic plasma cells in lymph nodes and spleen, reminiscent of MCD. More decisively, therapeutic antibodies that block IL-6 (siltuximab) or its receptor (tocilixumab) have demonstrated activity in controlling iMCD[11,42,43] and are now approved as frontline therapies. However, the cellular and anatomic source of IL-6 production in Castleman disease remains controversial. Early studies using immunohistochemistry on lymph node biopsies were suggestive of increased IL-6 within germinal centers in only a subset of cases of UCD or iMCD.[44,45] Subsequent immunohistochemical studies did not find IL-6 within germinal centers but rather showed positive IL-6 staining on plasma cells or endothelial cells.[46,47] More recent studies using a much more sensitive and specific *in-situ* hybridization assay on larger series of cases showed only minimal *IL6* mRNA expression in lymph nodes or lung biopsies involved by iMCD, mainly on rare stromal cells and/or endothelial cells.[48-50] Moreover, targeted next-generation sequencing or real-time polymerase chain reaction on tissue biopsies involved by iMCD did not show increased *IL6* transcripts compared to control tissues.[48,50] Our findings are consistent with the more recent evidence suggesting that IL-6 production might in fact not be increased within the enlarged lymph nodes, but could perhaps originate from another compartment such as bone marrow, circulating inflammatory leukocytes,[51] or endothelial cells.

Elevated serum VEGF levels are found in most patients with iMCD,[34] and VEGF has been previously proposed as a mediator of the increased lymph node vascularity in both UCD and iMCD.[52] In our study, *VEFGA* (*VEGF*) transcripts were only marginally increased in unicentric Castleman lymphadenopathy and not significantly increased in iMCD. Instead, we found that transcripts for *FLT1* (*VEGFR1*) and its less known ligand *PGF* were significantly increased in lymph nodes from both UCD and iMCD. PGF was first described as a placental angiogenic factor during embryogenesis, but was later shown to mediate angiogenesis in pathological inflammatory and ischemic processes in several other organs.[53] In addition, we found increased transcripts of Apelin receptor (*APLNR*) in both disease subtypes, and increased *APLN* transcripts in unicentric disease only. Similar to PGF signaling through FLT1, the APLN/APLNR system has been described as in important mediator of angiogenesis in pathological processes.[36] Thus, while systemic VEGF production might exert an effect on peripheral lymph nodes, our findings suggest that a role may exist for PGF/FLT1 and APLN/APLNR signaling as intrinsic angiogenic mediators in lymph nodes involved by Castleman disease.

While finalizing this manuscript, a targeted sequencing study of 2,003 autoimmunity-related genes on formalin-fixed/paraffin-embedded lymph nodes from patients with Castleman disease was published online.[50] The results of this study include findings suggestive of enrichment for transcripts of the complement and coagulation cascades, in addition to no demonstrable increase in *IL6* transcripts by targeted sequencing in Castleman disease compared to control lymph nodes. These unexpected findings are consistent with our results evaluating the entire transcriptome on fresh-frozen lymph node specimens, further supporting our conclusions.

Several limitations of our study need to be considered. First, we deliberately selected control lymph nodes with largely unremarkable cytomorphological features, in an attempt to capture gene expression patterns in Castleman disease that were different from “normal”. Thus, we were not able to study gene expression findings specific to Castleman disease, and absent in reactive lymphadenopathies with or without “Castleman-like” features. Second, our focus on specific gene sets was largely biased by our current understanding of Castleman disease, raising the possibility of other important findings in our dataset

not mentioned in this report but of potential biological relevance. Last, the power to detect differences in gene transcripts on surgically excised specimens might be limited by RNA degradation.

In summary, we provide the first description of the lymph node transcriptomes in UCD and iMCD, based on a small cohort of cases. Our findings raise the possibility of previously unrecognized disease mediators as potential therapeutic targets, such as elements of the complement cascade, CXCL13, and angiogenic signaling through FLT1 and APLNR. Future studies testing the contribution of individual upregulated genes and overrepresented pathways will be critical to building a better understanding of the pathogenesis of Castleman disease.

Disclosures

DCF has received research funding from EUSA Pharma for the ACCELERATE Registry, received consulting fees from EUSA Pharma, and received study drug from Pfizer for a clinical trial of sirolimus in Castleman disease. DCF holds a provisional patent and a pending patent for the diagnosis and treatment of Castleman disease. The remaining authors have no conflicts of interest to disclose.

Contributions

PH and AD designed the study; PH and RLK performed the histological review and selected the cases; PH analyzed the data and wrote the manuscript; AD, RLK, DCF and DJ contributed to the data analysis design and edited the manuscript; AD and DCF provided project support and expert knowledge.

Data-sharing statement

RNA sequencing data are available through NCBI GEO: GSE195477.

References

1. Dispenzieri A, Fajgenbaum DC. Overview of Castleman disease. Blood. 2020;135(16):1353-1364.
2. Gonzalez-Farre B, Martinez D, Lopez-Guerra M, et al. HHV8-related lymphoid proliferations: a broad spectrum of lesions from reactive lymphoid hyperplasia to overt lymphoma. Mod Pathol. 2017;30(5):745-760.
3. Dispenzieri A. POEMS syndrome: 2019 update on diagnosis, risk-stratification, and management. Am J Hematol. 2019;94(7):812-827.
4. Fajgenbaum DC, Uldrick TS, Bagg A, et al. International, evidence-based consensus diagnostic criteria for HHV-8-negative/idiopathic multicentric Castleman disease. Blood. 2017;129(12):1646-1657.
5. Fajgenbaum DC. Novel insights and therapeutic approaches in idiopathic multicentric Castleman disease. Blood. 2018;132(22):2323-2330.
6. Pierson SK, Stonestrom AJ, Shilling D, et al. Plasma proteomics identifies a 'chemokine storm' in idiopathic multicentric Castleman disease. Am J Hematol. 2018;93(7):902-912.
7. You L, Lin Q, Zhao J, Shi F, Young KH, Qian W. Whole-exome sequencing identifies novel somatic alterations associated with outcomes in idiopathic multicentric Castleman disease. Br J Haematol. 2020;188(5):e64-e67.
8. Li Z, Lan X, Li C, et al. Recurrent PDGFRB mutations in unicentric Castleman disease. Leukemia. 2019;33(4):1035-1038.
9. Nagy A, Bhaduri A, Shahmarvand N, et al. Next-generation sequencing of idiopathic multicentric and unicentric Castleman disease and follicular dendritic cell sarcomas. Blood Adv. 2018;2(5):481-491.
10. Chang KC, Wang YC, Hung LY, et al. Monoclonality and cytogenetic abnormalities in hyaline vascular Castleman disease. Mod Pathol. 2014;27(6):823-831.
11. van Rhee F, Wong RS, Munshi N, et al. Siltuximab for multicentric Castleman's disease: a randomised, double-blind, placebo-controlled trial. Lancet Oncol. 2014;15(9):966-974.
12. Kalari KR, Nair AA, Bhavsar JD, et al. MAP-RSeq: Mayo analysis pipeline for RNA sequencing. BMC Bioinformatics. 2014;15(1):224.
13. Liao Y, Smyth GK, Shi W. The Subread aligner: fast, accurate and scalable read mapping by seed-and-vote. Nucleic Acids Res. 2013;41(10):e108.
14. Benjamini Y, Hochberg Y. Controlling the false discovery rate: a practical and powerful approach to multiple testing. J R Stat Soc Series B Methodol. 1995;57(1):289-300.
15. Fontes M, Soneson C. The projection score--an evaluation criterion for variable subset selection in PCA visualization. BMC Bioinformatics. 2011;12(1):307.
16. Subramanian A, Tamayo P, Mootha VK, et al. Gene set enrichment analysis: a knowledge-based approach for interpreting genome-wide expression profiles. Proc Natl Acad Sci U S A. 2005;102(43):15545-15550.
17. Miller DV, Roden AC, Gamez JD, Tazelaar HD. Detection of C4d deposition in cardiac allografts: a comparative study of immunofluorescence and immunoperoxidase methods. Arch Pathol Lab Med. 2010;134(11):1679-1684.
18. Grogg KL, Attygalle AD, Macon WR, Remstein ED, Kurtin PJ, Dogan A. Expression of CXCL13, a chemokine highly upregulated in germinal center T-helper cells, distinguishes angioimmunoblastic T-cell lymphoma from peripheral T-cell lymphoma, unspecified. Mod Pathol. 2006;19(8):1101-1107.
19. Cartier A, Hla T. Sphingosine 1-phosphate: lipid signaling in pathology and therapy. Science. 2019;366(6463):eaar5551.
20. Cenci S. The proteasome in terminal plasma cell differentiation. Semin Hematol. 2012;49(3):215-222.
21. Jennewein MF, Alter G. The immunoregulatory roles of antibody glycosylation. Trends Immunol. 2017;38(5):358-372.
22. Price MJ, Patterson DG, Scharer CD, Boss JM. Progressive upregulation of oxidative metabolism facilitates plasmablast differentiation to a T-independent antigen. Cell Rep. 2018;23(11):3152-3159.
23. Saxton RA, Sabatini DM. mTOR Signaling in growth, metabolism, and disease. Cell. 2017;168(6):960-976.
24. Arenas DJ, Floess K, Kobrin D, et al. Increased mTOR activation in idiopathic multicentric Castleman disease. Blood. 2020;135(19):1673-1684.
25. Fajgenbaum DC, Langan RA, Japp AS, et al. Identifying and targeting pathogenic PI3K/AKT/mTOR signaling in IL-6-blockade-

refractory idiopathic multicentric Castleman disease. J Clin Invest. 2019;129(10):4451-4463.
26. Conway EM. Complement-coagulation connections. Blood Coagul Fibrinolysis. 2018;29(3):243-251.
27. Cohen D, Colvin RB, Daha MR, et al. Pros and cons for C4d as a biomarker. Kidney Int. 2012;81(7):628-639.
28. Wiedermann CJ. Secretoneurin: a functional neuropeptide in health and disease. Peptides. 2000;21(8):1289-1298.
29. Castello LM, Raineri D, Salmi L, et al. Osteopontin at the crossroads of inflammation and tumor progression. Mediators Inflamm. 2017;2017:4049098.
30. Lund SA, Giachelli CM, Scatena M. The role of osteopontin in inflammatory processes. J Cell Commun Signal. 2009;3(3-4):311-322.
31. Del Prete A, Scutera S, Sozzani S, Musso T. Role of osteopontin in dendritic cell shaping of immune responses. Cytokine Growth Factor Rev. 2019;50:19-28.
32. Vermi W, Lonardi S, Bosisio D, et al. Identification of CXCL13 as a new marker for follicular dendritic cell sarcoma. J Pathol. 2008;216(3):356-364.
33. Yu H, Shahsafaei A, Dorfman DM. Germinal-center T-helper-cell markers PD-1 and CXCL13 are both expressed by neoplastic cells in angioimmunoblastic T-cell lymphoma. Am J Clin Pathol. 2009;131(1):33-41.
34. Liu AY, Nabel CS, Finkelman BS, et al. Idiopathic multicentric Castleman's disease: a systematic literature review. Lancet Haematol. 2016;3(4):e163-175.
35. Rahimi N. VEGFR-1 and VEGFR-2: two non-identical twins with a unique physiognomy. Front Biosci. 2006;11:818-829.
36. Wu L, Chen L, Li L. Apelin/APJ system: a novel promising therapy target for pathological angiogenesis. Clin Chim Acta. 2017;466:78-84.
37. Cumpelik A, Heja D, Hu Y, et al. Dynamic regulation of B cell complement signaling is integral to germinal center responses. Nat Immunol. 2021;22(6):757-768.
38. Havenar-Daughton C, Lindqvist M, Heit A, et al. CXCL13 is a plasma biomarker of germinal center activity. Proc Natl Acad Sci U S A. 2016;113(10):2702-2707.
39. Oksenhendler E, Carcelain G, Aoki Y, et al. High levels of human herpesvirus 8 viral load, human interleukin-6, interleukin-10, and C reactive protein correlate with exacerbation of multicentric castleman disease in HIV-infected patients. Blood. 2000;96(6):2069-2073.
40. Brandt SJ, Bodine DM, Dunbar CE, Nienhuis AW. Dysregulated interleukin 6 expression produces a syndrome resembling Castleman's disease in mice. J Clin Invest. 1990;86(2):592-599.
41. Suthaus J, Stuhlmann-Laeisz C, Tompkins VS, et al. HHV-8-encoded viral IL-6 collaborates with mouse IL-6 in the development of multicentric Castleman disease in mice. Blood. 2012;119(22):5173-5181.
42. Beck JT, Hsu SM, Wijdenes J, et al. Brief report: alleviation of systemic manifestations of Castleman's disease by monoclonal anti-interleukin-6 antibody. N Engl J Med. 1994;330(9):602-605.
43. Nishimoto N, Kanakura Y, Aozasa K, et al. Humanized anti-interleukin-6 receptor antibody treatment of multicentric Castleman disease. Blood. 2005;106(8):2627-2632.
44. Yoshizaki K, Matsuda T, Nishimoto N, et al. Pathogenic significance of interleukin-6 (IL-6/BSF-2) in Castleman's disease. Blood. 1989;74(4):1360-1367.
45. Leger-Ravet MB, Peuchmaur M, Devergne O, et al. Interleukin-6 gene expression in Castleman's disease. Blood. 1991;78(11):2923-2930.
46. Post GR, Bell RC, Rjoop A, Lobo RH, Yuan Y, Post SR. Diagnostic utility of interleukin-6 expression by immunohistochemistry in differentiating Castleman disease subtypes and reactive lymphadenopathies. Ann Clin Lab Sci. 2016;46(5):474-479.
47. Lai YM, Li M, Liu CL, et al. [Expression of interleukin-6 and its clinicopathological significance in Castleman's disease]. Zhonghua Xue Ye Xue Za Zhi. 2013;34(5):404-408.
48. Otani K, Inoue D, Fujikura K, et al. Idiopathic multicentric Castleman's disease: a clinicopathologic study in comparison with IgG4-related disease. Oncotarget. 2018;9(6):6691-6706.
49. Kinugawa Y, Uehara T, Iwaya M, et al. IL-6 expression helps distinguish Castleman's disease from IgG4-related disease in the lung. BMC Pulm Med. 2021;21(1):219.
50. Wing A, Xu J, Meng W, et al. Transcriptome and unique cytokine microenvironment of Castleman disease. Mod Pathol. 2022;35(4),451–461.
51. Ishiyama T, Nakamura S, Akimoto Y, et al. Immunodeficiency and IL-6 production by peripheral blood monocytes in multicentric Castleman's disease. Br J Haematol. 1994;86(3):483-489.
52. Nishi J, Maruyama I. Increased expression of vascular endothelial growth factor (VEGF) in Castleman's disease: proposed pathomechanism of vascular proliferation in the affected lymph node. Leuk Lymphoma. 2000;38(3-4):387-394.
53. Skoda M, Stangret A, Szukiewicz D. Fractalkine and placental growth factor: a duet of inflammation and angiogenesis in cardiovascular disorders. Cytokine Growth Factor Rev. 2018;39:116-123.